Supporting Information

Close-packed ultra-smooth self-assembled monolayer of $CsPbBr_3$ perovskite nanocubes

Biplab K. Patra,[†#π] Harshal Agrawal,[†#] Jian-Yao Zheng,[†] Xun Zha,[‡] Alex Travesset[¥] and Erik C. Garnett[†*]

[†]Center for Nanophotonics, AMOLF, Amsterdam, The Netherlands

[π]Materials Chemistry Department, CSIR-Institute of Minerals and Materials Technology, Bhubaneswar 751013, India

[‡]Department of Physics and Astronomy, Iowa State University, Ames, Iowa 50011, United States

[¥]Department of Physics and Astronomy and Ames Lab, Iowa State University, Ames, Iowa 50011, United States

A) Experimental set-up and characteristics of the monolayer self-assembly.

We make close-packed monolayer of nanocubes by controlled evaporation of toluene droplets on silicon (Si) substrate of about 5x5 mm in a closed chamber. First, we clean the Si substrate using soap solution and then put into IPA solution for sonication at 100 W for 10 min. After that we blow dried the IPA from the substrate and plasma cleaned using 100 W ozone plasma cleaner for 30 sec. Then the substrate is soaked with toluene for 10 min by dipping it into toluene to get a nice wetting of nanocubes solution. This substrate has been used for making monolayer self-assembly.

10 µl of the cube solution is dropcast on plasma treated silicon substrate and a beaker containing toluene has been placed near it. The whole system is then covered immediately with a glass container. Evaporation of nanocube solution will be slowed down

by the excess toluene vapor inside thus forming controlled assembly. Details of the setup are shown in figure 1 in main text.

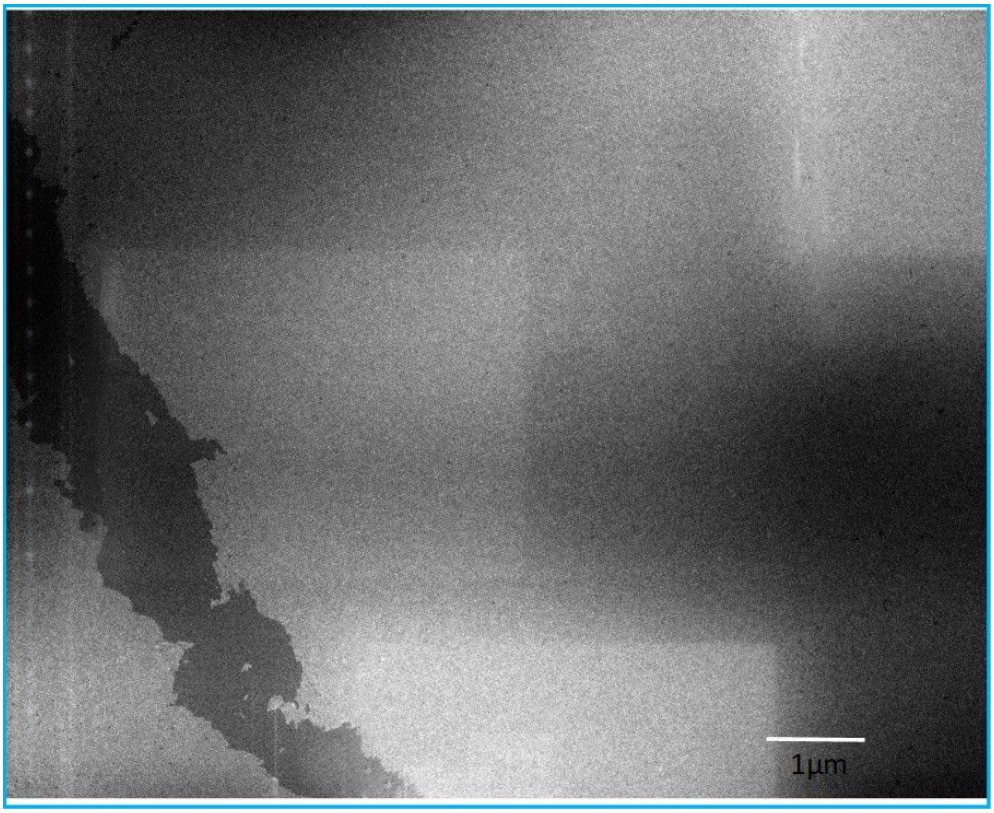

Figure S1: SEM image of self-assembly of $CsPbBr_3$ Nanocubes.

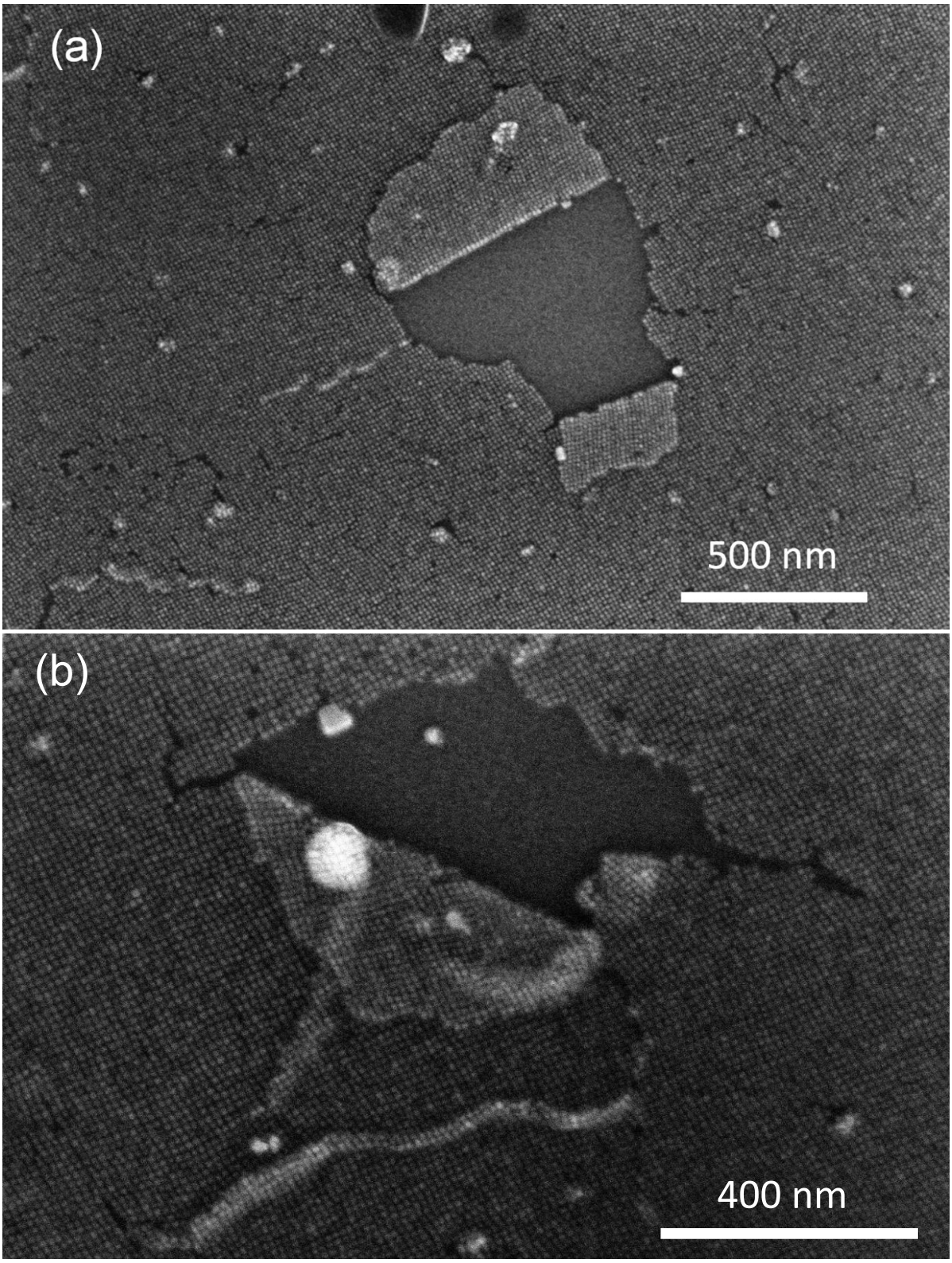
(a)
500 nm
(b)
400 nm

Figure S2: The cleaning procedure (rinse one time with methyl acetate solution very gently) used to avoid charging effects during SEM led to partial delamination in a few places (figure S2 a-b) clearly indicates that the assembled film is a monolayer.

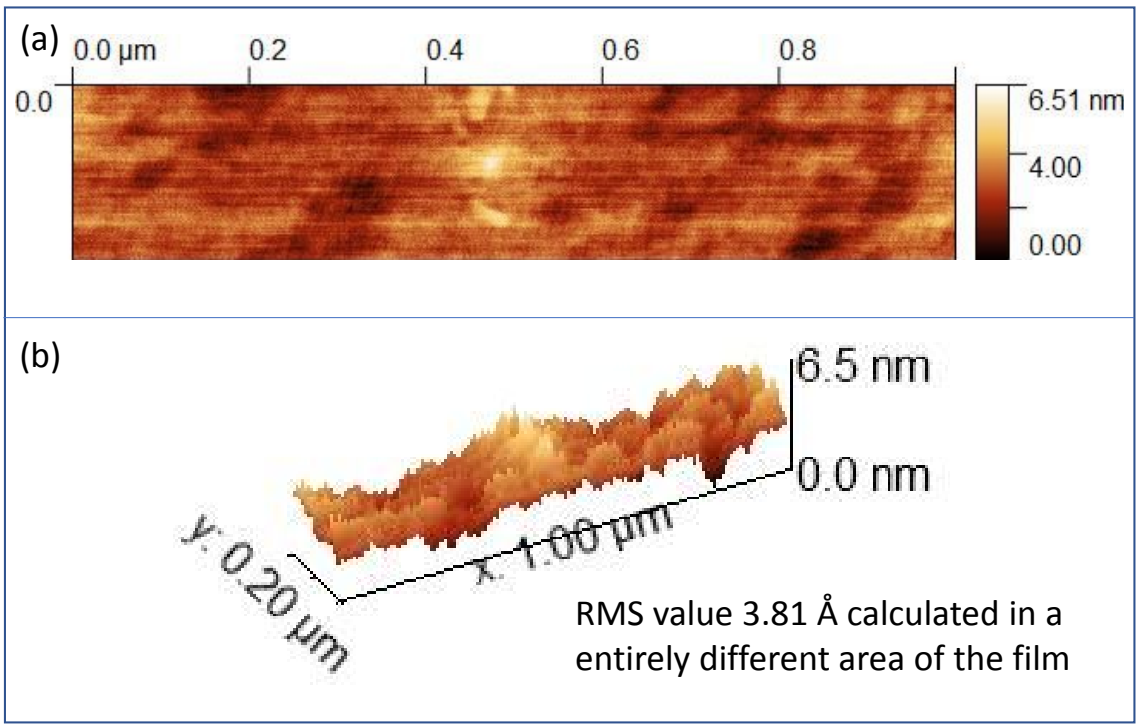

Figure S3: (a) AFM scan of an entirely different area from the area shown in the main text to measure the surface roughness. (b) Corresponding 3D profile of the measured area with calculated RMS value.

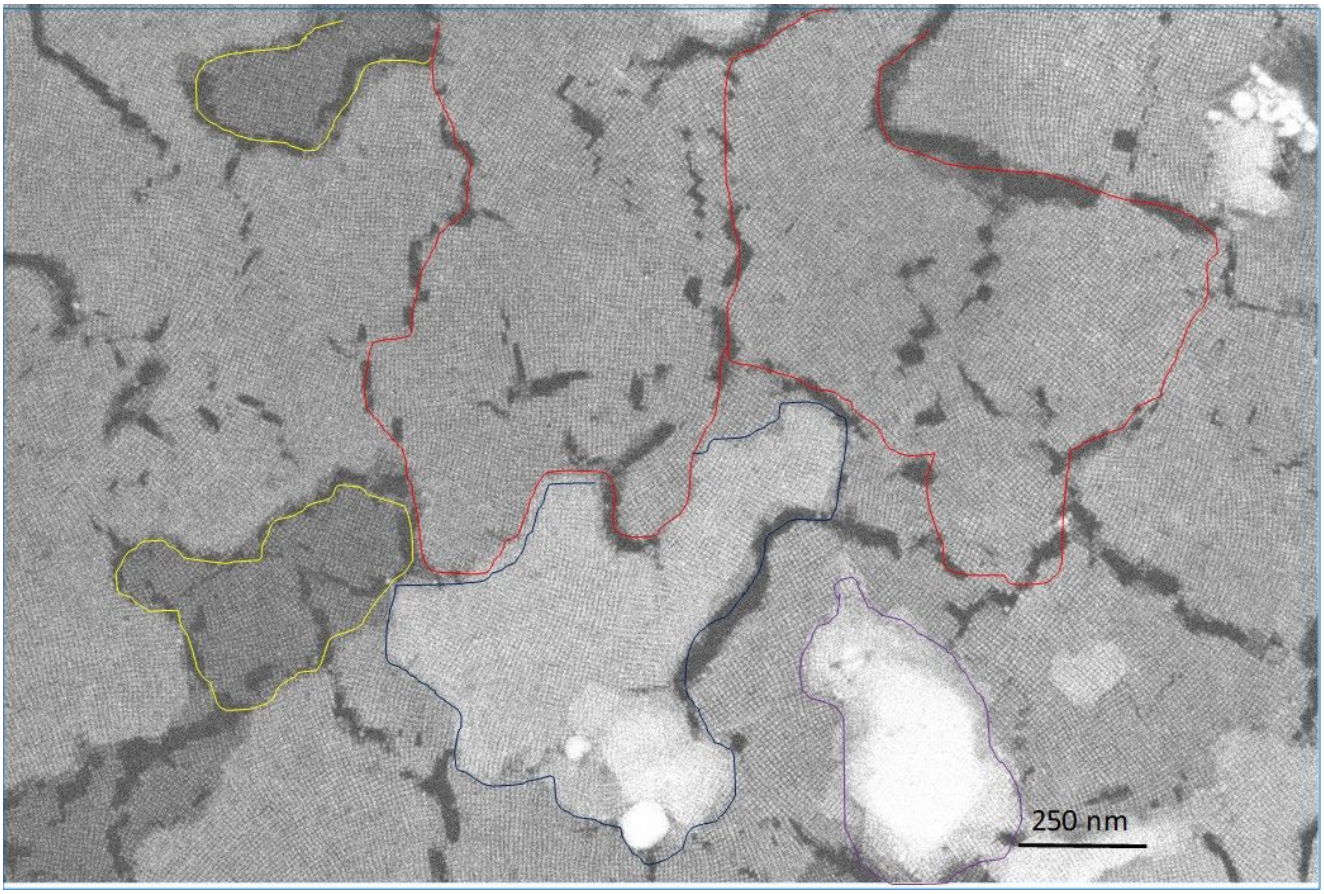

Figure S4: SEM image of multiple layers self-assembly of as synthesized perovskite nanocubes taken using an in-Column Detector (ICD) in SEM. Contrast differences in different areas indicate the multiple layer stacking of nanocube assembly. Yellow area single layer, red area double layer, blue area triple layer and purple area show multiple layer stacking of nanocube assembly.

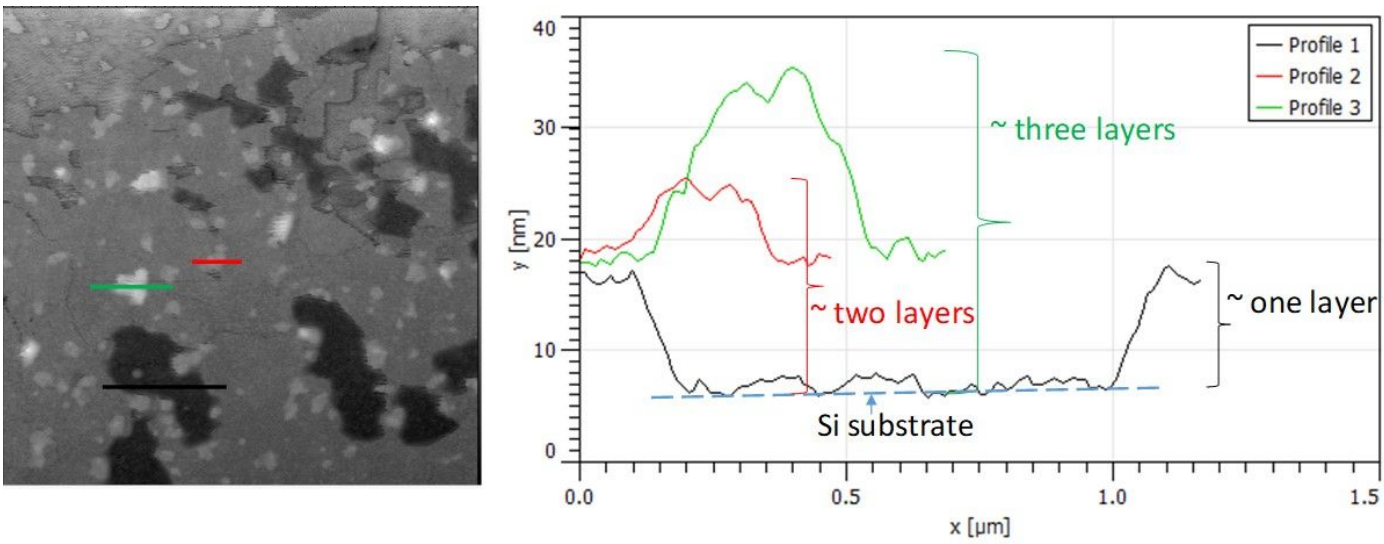

Figure S5: AFM image of the multiple layers stacking of nanocube assembly (left panel). Right panel shows height profile and the estimated number of layers.

B) Absorption, PL and PL quantum yield (PLQY) measurement.

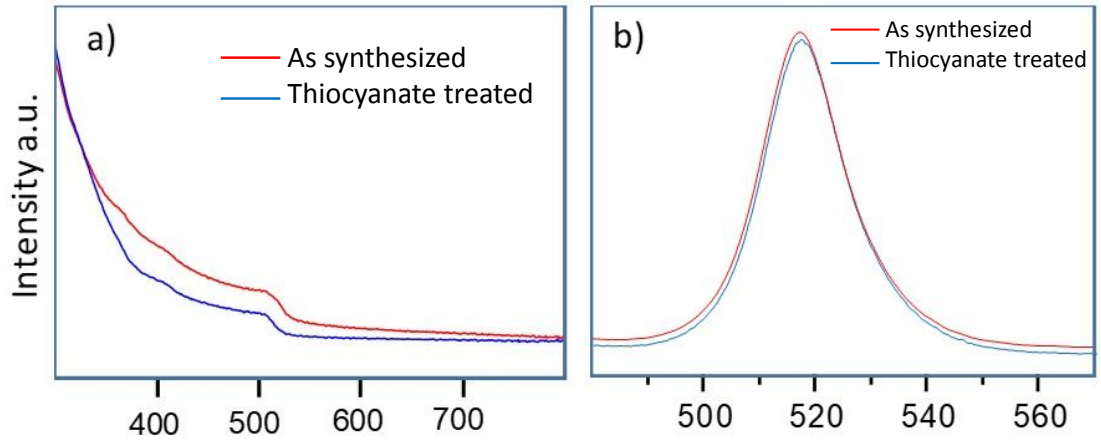

Figure S6: a) UV-VIS absorption spectra b) Photoluminescence (PL) spectra of as synthesized sample and thiocyanate treated sample.

A custom-built, 10 cm diameter integrating sphere manufactured by Labsphere was used. The sample cuvette was mounted at the center of the integrating sphere, as shown in figure S7. Light from the laser (Thorlabs, L405P20, 405 nm) was incident onto the sample

through a small hole in the sphere wall. The laser was modulated by optical chopper (Thorlabs, MC2000B-EC) and the intensity was controlled with neutral density filters (Thorlabs). A diffusely reflecting baffle was positioned between the sample and the exit port in order to prevent luminescence from reaching the detector directly. The laser beam hit the sample within a cylindrical cuvette.

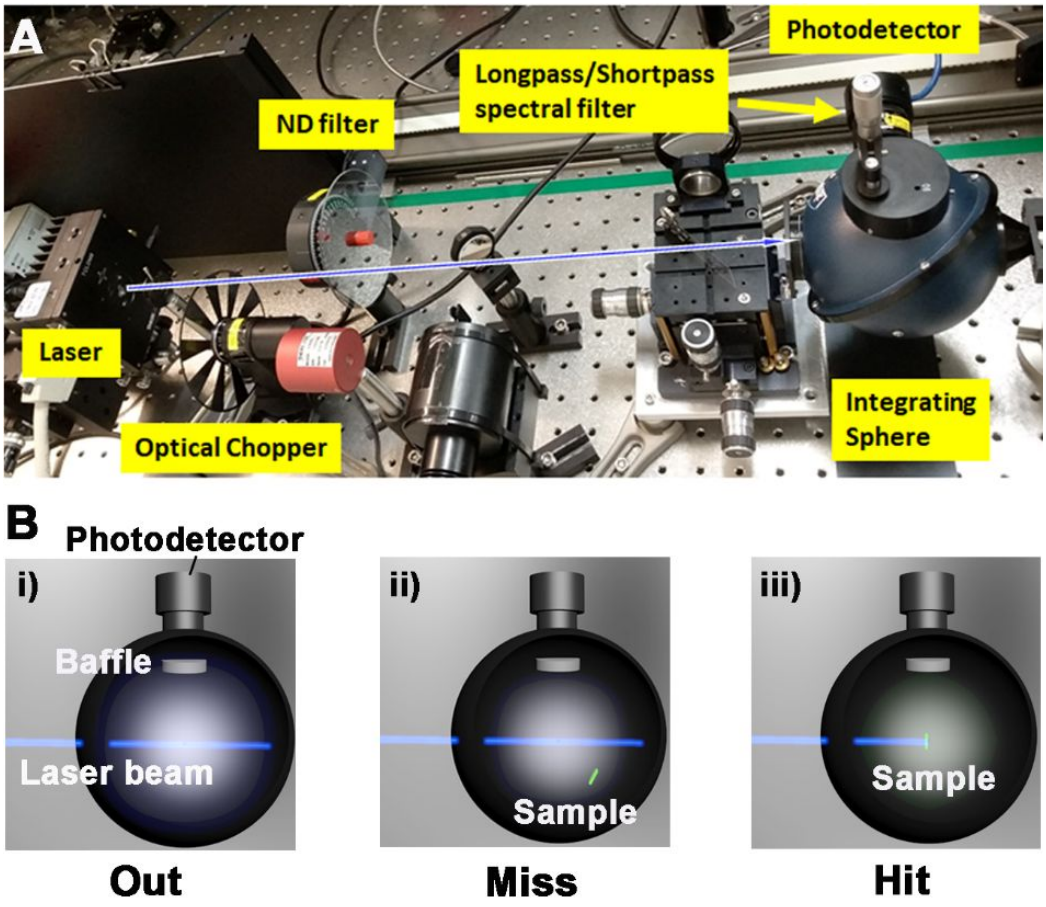

Figure S7. (A) The experimental setup for the PLQY measurement. (B) Diagram illustrating the three configurations of the sphere required for the PLQY measurement: i) the sphere is empty; ii) the sample is in place and the laser beam is directed onto the sphere wall; iii) the sample is in place and the laser beam is directed onto the sample.

Light leaving the exit port of the sphere, hits onto low-noise Newport 818-SL calibrated photodetector which is connected to Stanford Research Systems SR830 lock-in amplifier. We measure the excitation and emission separately by using a short pass filter (Thorlabs FESH0450) and long pass filter (Thorlabs FELH0450) in front of the photodetector. The sensitivity as a function of wavelength is calibrated with the spectral responsivity of photodetector. The PLQY was calculated according to the method outlined by de Mello.[8] PLQY (η_{PL}) is given by:

$$\eta_{PL} = \frac{P_c(\lambda) - (1 - A)P_b(\lambda)}{L_a(\lambda)A} \quad (1)$$

Where A = $\frac{L_b(\lambda) - L_c(\lambda)}{L_b(\lambda)}$ (2)

According to this notation, $P_c(\lambda)$ and $P_b(\lambda)$ are the luminescence as a result of direct excitation of the sample and secondary excitation, respectively. The latter emission is due to the reflected excitation light from sphere walls hitting the sample. The notation A is the absorbance of the sample. $L_a(\lambda)$ is the excitation profile for an empty sphere, $L_b(\lambda)$ is the excitation when the excitation light first hits the sphere wall, and $L_c(\lambda)$ is the excitation when the sample is directly excited.

The outputs from photodetector were read out by Stanford Research Systems SR830 lock-in amplifiers. After calibration with the spectral responsivity of photodetector, the data are summarized in table S1. For the untreated $CsPbBr_3$ nanocubes, the PLQY is calculated to be 72.9%. After the ligand exchange, the PLQY is increased to 90.9%.

Readout from photodetector after calibration (nA)				
Untreated $CsPbBr_3$ nanocubes	L_a	L_b	L_c	***A***
	22.66	22.37	6.02	73.1%
	P_b	P_c		η_{PL}
	0.32	12.16		72.9%
Treated $CsPbBr_3$ nanocubes	L_a	L_b	L_c	***A***
	22.24	21.52	5.35	75.1%
	P_b	P_c		η_{PL}
	0.47	15.30		90.9%

Table S1: Readout from the photodetector after calibration with the spectral responsivity of photodetector and the calculated absorption coefficient (***A***) and η_{PL} (PLQY).

C) Modelling of $CsPbBr_3$ nanocubes analyzed in our calculations.

The nanocube core consists of a perovskite with chemical composition $CsPbBr_3$ structure defined in figure S8. The following molecules ($-NH_3^+$, $-COO^-$, $-NH^{4+}$, $-SCN^-$) are modeled as rigid bodies. The molecules oleyl ammonium (OAm^+), oleate (OA^-), SCN^- contain some flexible elements. We consider two different types of nanocubes, with and without oleyl chains, as depicted in figure S8. The ligands are bound electrostatically to the perovskite core through the Br^- and Cs^+ ions. The core consists of many Perovskite unit cells with a 0.587 nm lattice constant, and it is built as a rigid cube with the same mass and moment of inertia of the $CsPbBr_3$ bulk atom constituents. The bulk atoms are not simulated since we consider a hollow core, but with the equivalent mass and moment of inertia. The CH_2, CH_3, NH_3 and NH_4 groups are modeled as united atoms. The force field parameters are taken from the OPLS force field, resorting to CHARMM when unavailable.[2,3]

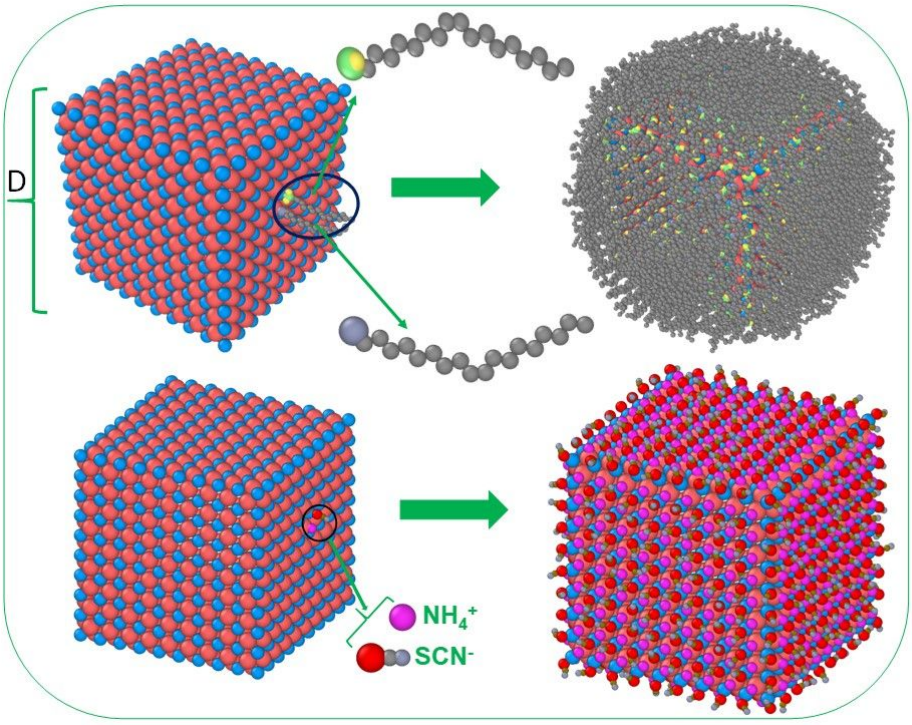

Figure-S8: A 5.283 nm $CsPbBr_3$ Perovskite nanocube with OAm^+ (blue headed oleate $C_{18}H_{35}NH_3^+$) and OA^- (green and yellow headed oleate $C_{18}H_{33}O_2^-$) are shown in the top panel while SCN^- and head group NH^{4+} are shown in the bottom panel. OA^- and SCN^- find to bind cationic sites of Cs^+ for (100) exposed facets and Pb^{2+} for (200) exposed facets (for simplicity we consider Cs^+ is at the surface binding sites throughout the calculations). Whereas OAm^+ and NH^{4+} are attached on Br^- sites. We assume all OAm^+ is replaced from the surface during NH_4SCN treatment by NH^{4+} during the calculations for simplicity although in real experiment replacement occurs partially which is demonstrated from the fact that after treatment the nanocubes still can make stable dispersion in nonpolar solvent.

The lattice constant a_{nn} is varied in the interval $\left[a_{nn}^{min}, a_{nn}^{max}\right]$ as shown in table S2. We consider a simple square (ss) planar superlattice consisting of a 4x4 nanocubes, with periodic boundary conditions, as shown in figure S9.

Name	n_{unit}	*D (nm)*	a_{nn} (oleate)	a_{nn} (SCN^-)
N2	2	1.17	[2.5, 5.1]	[2.1, 2.8]
N7	7	4.11	[7,.2 9.5]	[5.1, 6.2]

N9	9	5.28	[8.7, 10.6]	[6.2, 7.4]
N11	11	6.46	[10.4, 12.0]	[7.4, 8.4]
N13	13	7.63	[11.8, 13.1]	[8.6, 9.5]

Table S2: Summary of the nanocubes analyzed. n_{unit} is the number of unit cells along the linear dimension. D is the size of the nanocubes and a_{nn} the lattice constant, see figures S8, S9.

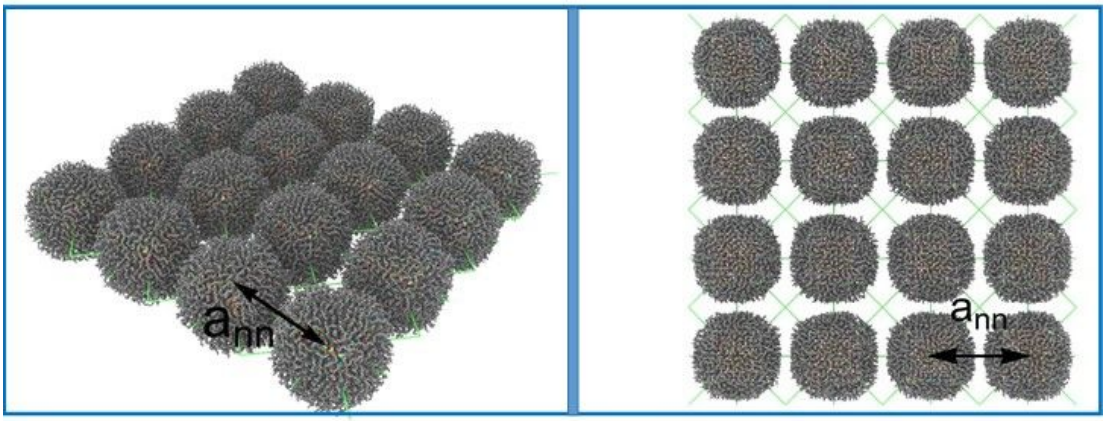

Figure S9: Snapshot of a 4x4 square superlattice in two different view. The lattice constant a_{nn} is shown.

D) Free energy calculation.

Following previous work,[4] the free energy is calculated by integration of pressure over volume,

$$\mathrm{F} = -\int_{\mathrm{a}}^{\mathrm{a}_\infty} P dV \qquad (3)$$

where the cubes are held stable by placing extra harmonic springs connecting their centers.

We run NVT simulations for the superlattice starting from lattice constant a_{nn}^{max} much larger than r_0, the equilibrium distance that is a minimum of the free energy, to a lattice constant

$a_{nn}^{min} < r_0$. Note that the lattice constant of the corresponding simple square lattice is the same as the center-to-center distance of neighboring nanocubes. We collect the pressure at each lattice constant and obtain the equation of state (*P(V)*) through a polynomial fit, which is integrated versus the volume to obtain the free energy, as described in literature.[4] The equilibrium distance r_0 (between nanocube centers) is the lattice constant (of the superlattice) that minimizes the free energy, which occurs when the pressure becomes zero.

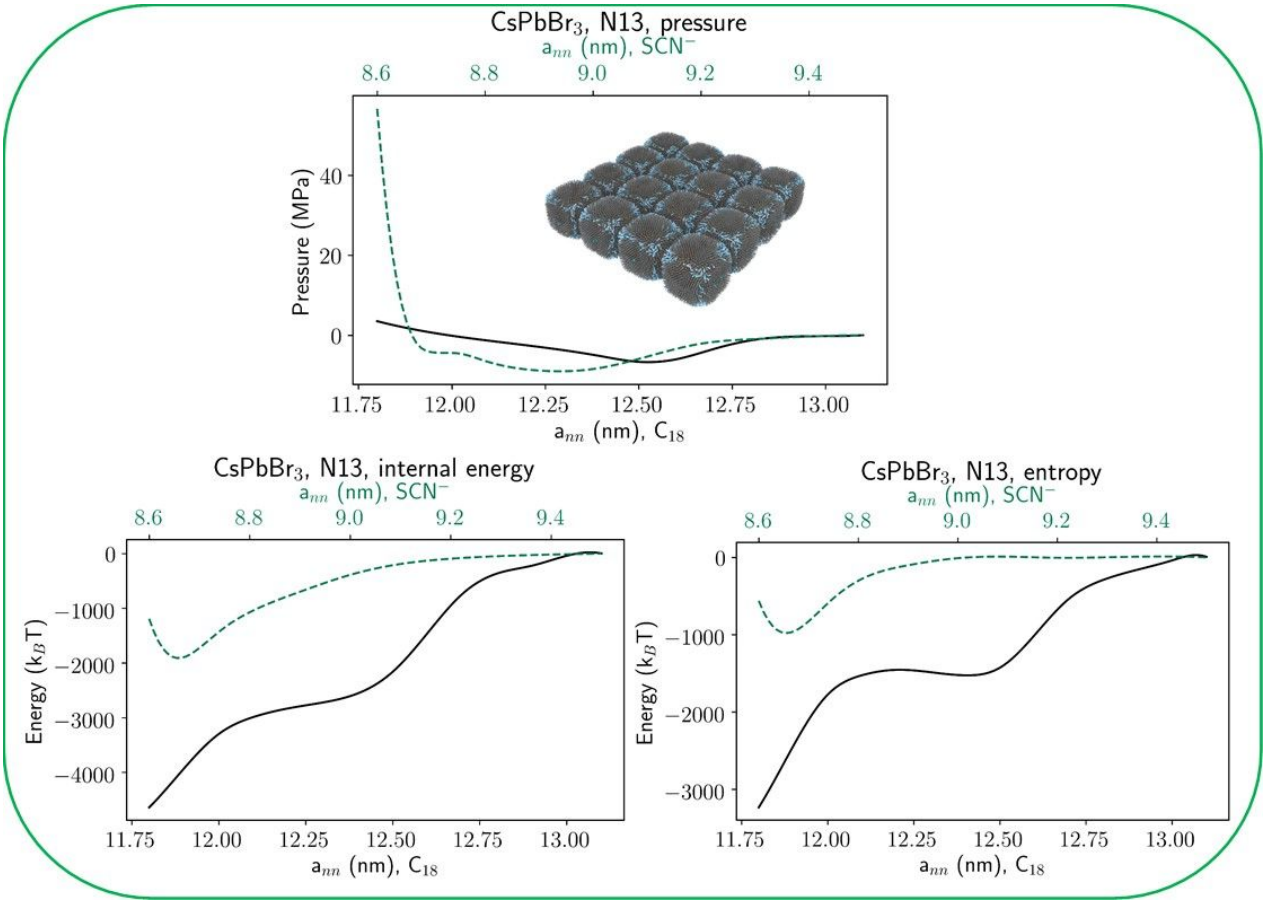

Figure S10: Calculated internal energy, entropy and pressure of the square lattice. A representative image of the lattice with oleyl chains grafted nanocube is shown in the inset of pressure plot.

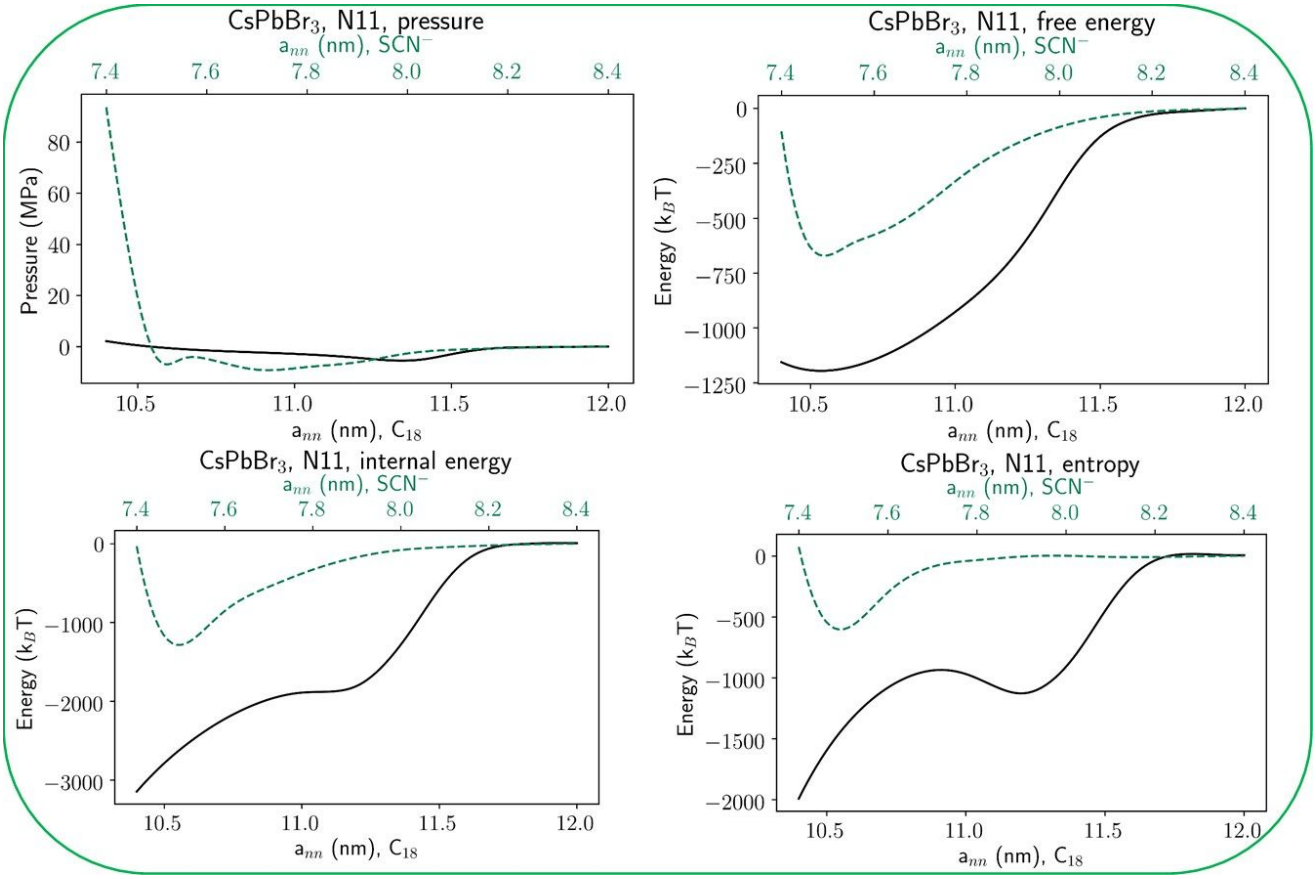

Figure S11: Calculated pressure, free energy F_0 (oleate)=-1195K_BT & F_0 (Thiocyanate)=-673K_BT, internal energy and entropy of the square lattice for N11.

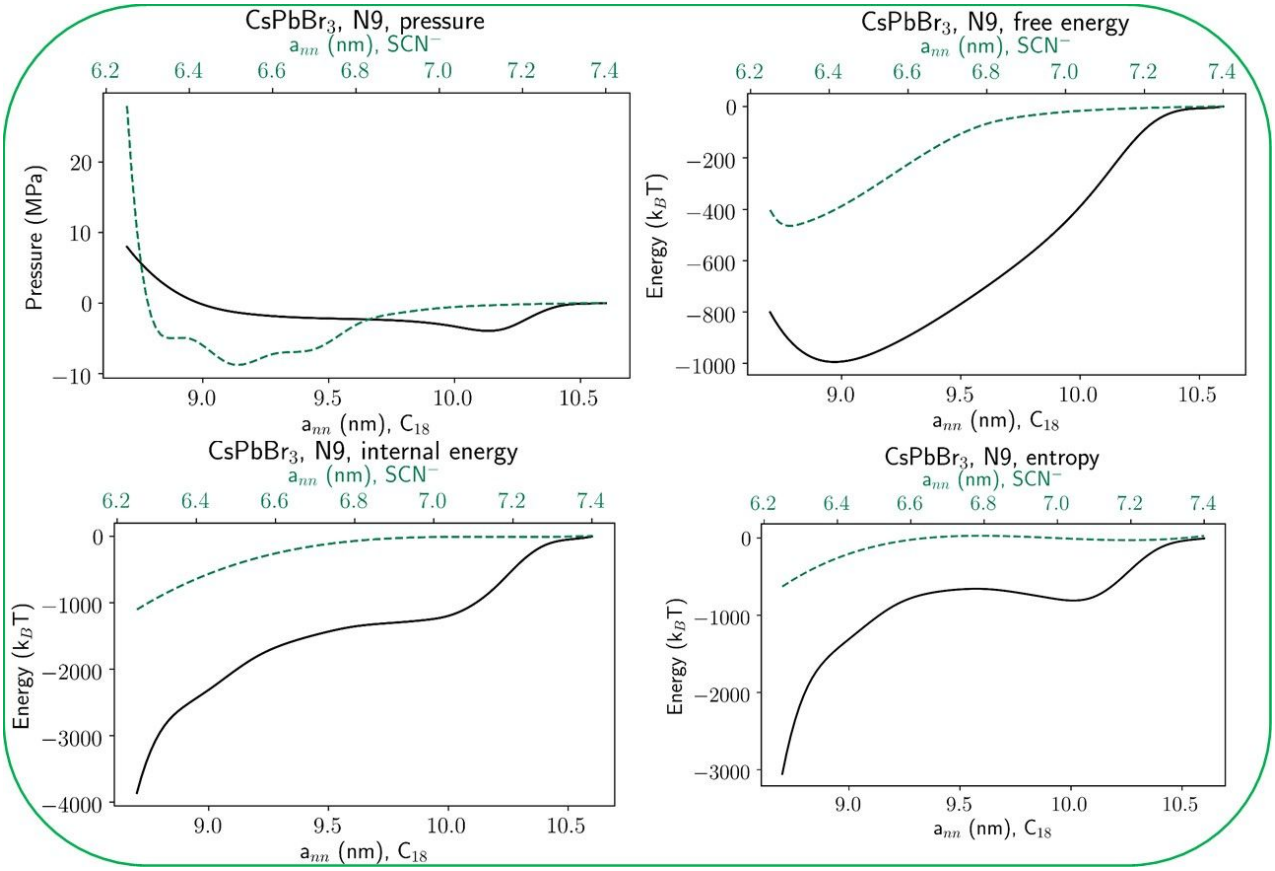

Figure S12: Calculated pressure, calculated free energy F_0(oleate)=-995K_BT & F_0(Thiocyanate)=-465K_BT], internal energy, and entropy of the square lattice for N9.

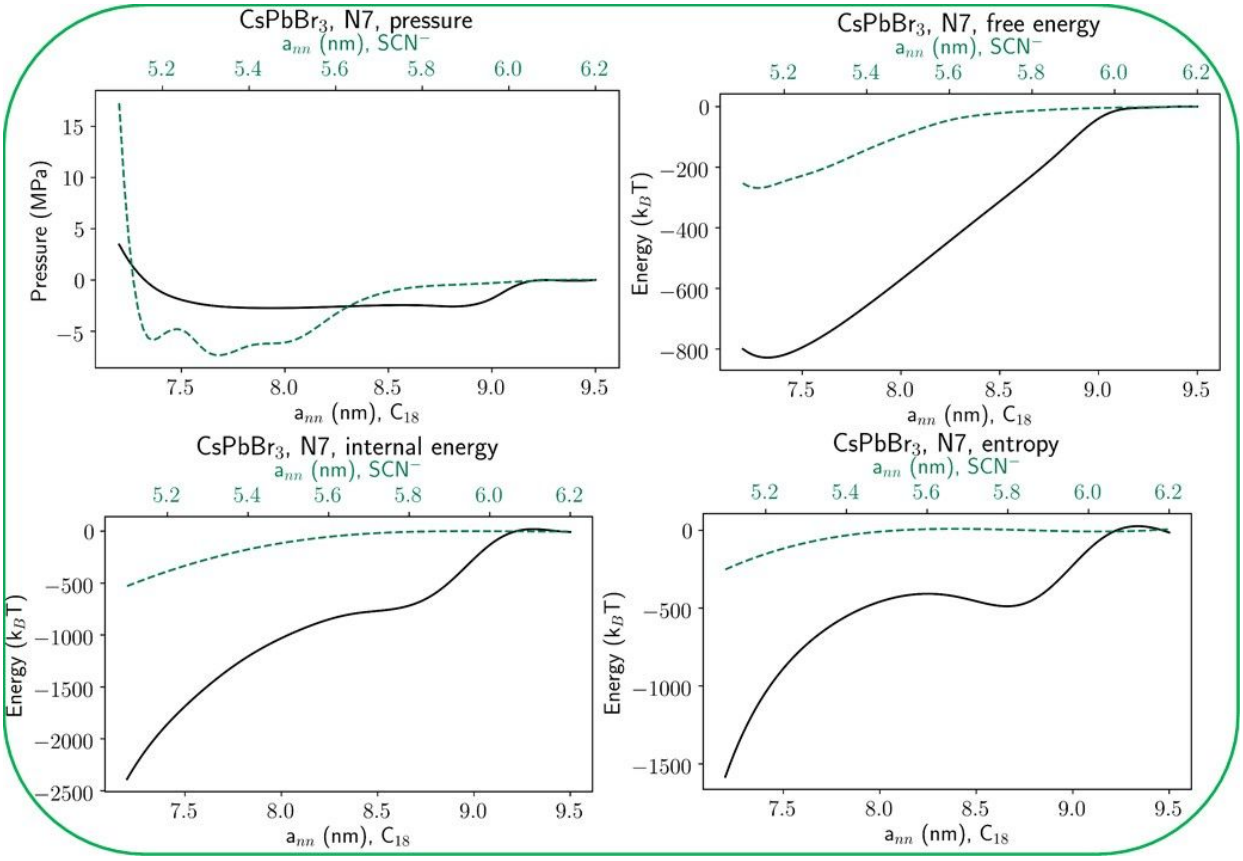

Figure S13: Calculated pressure, calculated free energy F_0(oleate)=-829K_BT] & F_0(Thiocyanate)=-270K_BT], internal energy, entropy of the square lattice N7.

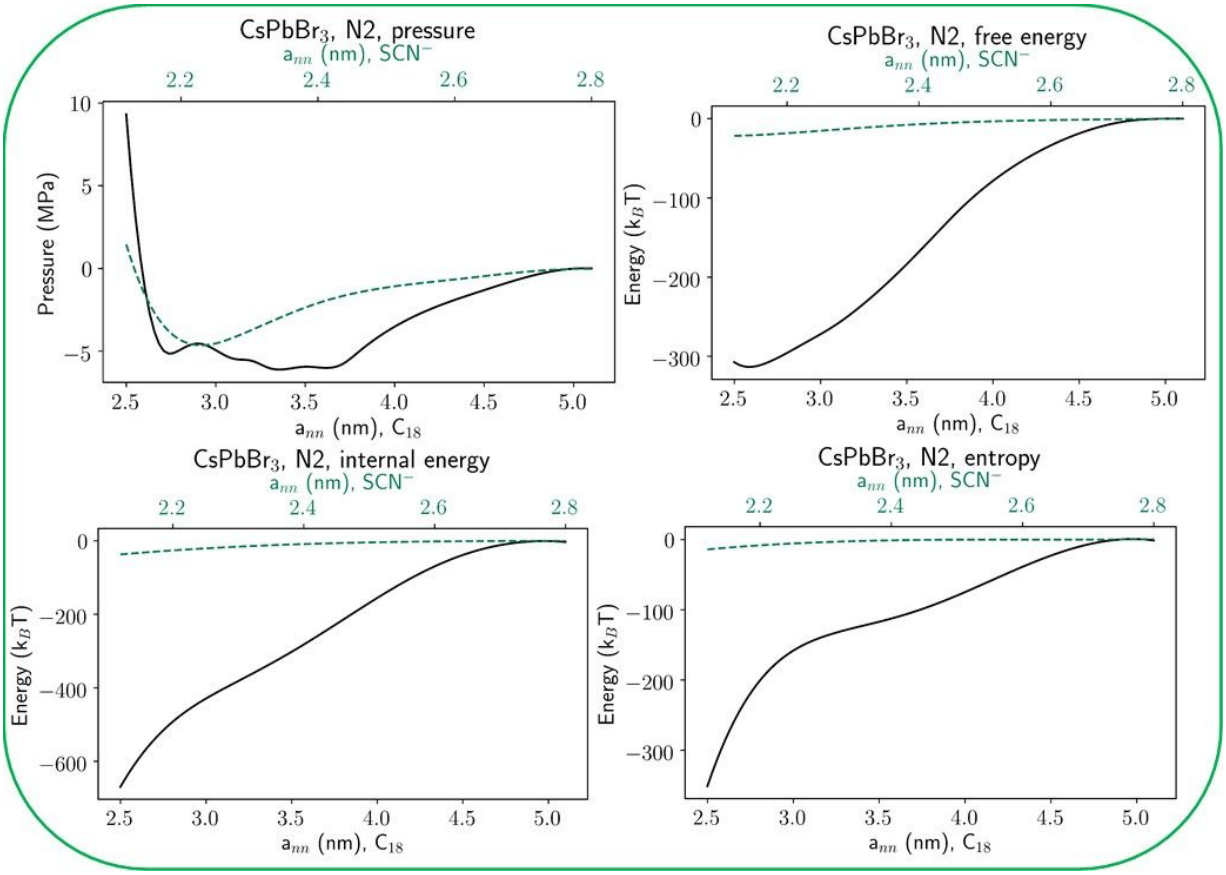

Figure S14: Calculated pressure, calculated free energy F_0(oleate)= -314K_BT] & F_0(Thiocyanate)=-21K_BT], internal energy, entropy of the square lattice for N2.

E) Calculation of equilibrium separation between two nanocubes in a superlattice.

We follow previous work[5–7] and develop analytical formulas for the nanocube equilibrium separation r_0.

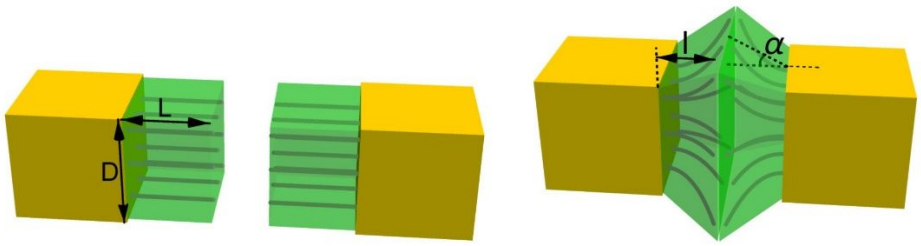

Figure S15: The fully stretched chain and the compressed chain.

The maximum extended length for a chain containing *n* hydrocarbons is[5] *L=0.12(n+1)*. There is also an additional group, either -COO^- or -NH_3^+, which we approximate as an additional carbon, so we will use the formula

$$L \approx 0.12(n+2) \quad (4)$$

which for *n=16*, gives *L=2.16* nm. The molecular area A_0, related to the grafting density as $\sigma = \frac{1}{A_0}$, is given by $A_0 = \frac{a_0^2}{2} = 0.172\text{nm}^2$, where a_0 is the lattice constant of the perovskite $CsPbBr_3$ unit cell. In the limit of a very large nanocube, $\frac{D}{L} \to \infty$, we expect that the chains will be maximally stretched, and the lattice constant $a_{nn}=r_0$, will be given by

$$r_0^\infty = D + 2L \text{ or } \frac{r_0^\infty - D}{2L} = 1 \quad (5)$$

The equilibrium lattice constant r_0 at finite *D* can be calculated by assuming that the chains splay from the edges of the cube at an angle α, leading to an effective area

$$A = \frac{1}{3}\left(D^2 + (D + 2Lsin(\alpha))^2 + D(D + 2Lsin(\alpha))\right) \approx A_0\left(1 + 2sin(\alpha)\frac{L}{D}\right) \quad (6)$$

where we have assumed that the effective area is defined as that of a truncated cone whose small base is D^2 and whose large base is $(D + 2Lsin(\alpha))^2$. Then, assuming the incompressibility of the hydrocarbon chains, we have the equation $Ar_0 = A_0 r_0^\infty$, leading to

$$r_0 = \frac{D + 2L}{1 + 2sin\,(\alpha)\frac{L}{D}} \tag{7}$$

which leads to $r_0 = r_0^{\infty}$ for $\lambda = \frac{L}{D} \to \infty$. Equation 7 shows better agreement with the simulation result as the nanocube becomes bigger (larger λ), as shown in figure S16.

In regards of the minimum of the free energy (F_0) it is our expectation that it should grow with the area of the core D^2, hence

$$F_0(D) \approx f_0 D^2 \tag{8}$$

The fit in figure S16 shows that this formula is well satisfied. The resulting coefficient is also given in table S3.

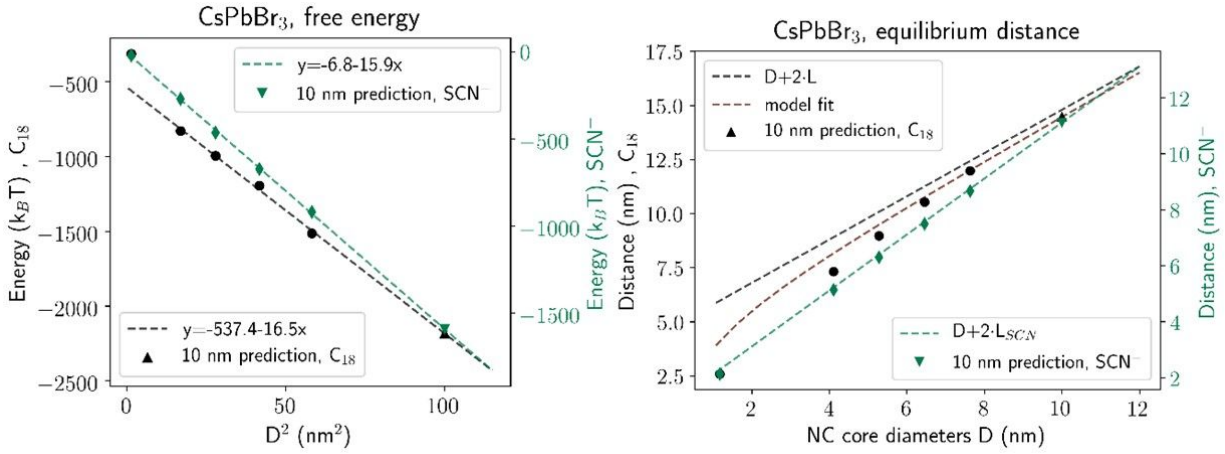

Figure S16: Free energy and equilibrium distance per NC of square superlattice, with nanocubes capped with oleyl chains and SCN^-, as a function of the nanocube diameters D. We use L=2.4 nm for the oleyl chains, and L=0.556 nm the for SCN^- ligand.

Name	$\lambda = L/D$	r_0 (C_{18})	F_0 (C_{18})	$\lambda = L/D$	r_0 (SCN^-)	F_0 (SCN^-)
N2	2.04	2.59	-314	0.47	2.13	-21
N7	0.59	7.32	-829	0.14	5.13	-270

N9	0.46	8.97	-995	0.11	6.30	-465
N11	0.37	10.53	-1195	0.09	7.49	-673
N13	0.31	11.98	-1514	0.07	8.66	-920
f_0			-16.5			-15.9

Table S3: Summary of the equilibrium separation and free energy. Units of length are in nm, units of energy are k_BT.

References

(1) Malaquin, L.; Kraus, T.; Schmid, H.; Delamarche, E.; Wolf, H. Controlled Particle Placement through Convective and Capillary Assembly. *Langmuir* **2007**, *23*, 11513–11521.

(2) Jorgensen, W. L.; Maxwell, D. S.; Tirado-Rives, J. Development and Testing of the OPLS All-Atom Force Field on Conformational Energetics and Properties of Organic Liquids. *J. Am. Chem. Soc.* **1996**, *118*, 11225–11236.

(3) Brooks, B. R.; Bruccoleri, R. E.; Olafson, B. D.; States, D. J.; Swaminathan, S.; Karplus, M. CHARMM: A Program for Macromolecular Energy, Minimization, and Dynamics Calculations. *J. Comput. Chem.* **1983**, *4*, 187–217.

(4) Zha, X.; Travesset, A. Stability and Free Energy of Nanocrystal Chains and Superlattices. *J. Phys. Chem. C* **2018**, *122*, 23153–23164.

(5) Landman, U.; Luedtke, W. D. Small Is Different: Energetic, Structural, Thermal, and Mechanical Properties of Passivated Nanocluster Assemblies. *Faraday Discuss.* **2004**, *125* , 1–22.

(6) Travesset, A. Nanoparticle Superlattices as Quasi-Frank-Kasper Phases. *Phys.*

Rev. Lett. **2017**, *119*, 1–5.

(7) Travesset, A. Topological Structure Prediction in Binary Nanoparticle Superlattices. *Soft Matter* **2017**, *13*, 147–157.

(8) J. C. de Mello, H. F. Wittmann, R. H. Friend, An Improved Experimental Determination of External Photoluminescence Quantum efficiency. *Adv*. *Mater*. **1997**, *9*, 230.